Journal of Materials Chemistry C

PAPER

View Article Online
View Journal | View Issue

Cite this: J. Mater. Chem. C, 2014, 2, 3717

Direct synthesis of graphene quantum dots on hexagonal boron nitride substrate

Xuli Ding*[ab]

Received 13th February 2014
Accepted 12th March 2014

DOI: 10.1039/c4tc00298a

www.rsc.org/MaterialsC

We report the fabrication and characterization of large-scale graphene quantum dots (GQDs) grown on hexagonal boron nitride (h-BN) substrates with different layers and similar size of island diameters. The GQDs on h-BN synthesized by chemical vapor deposition (CVD) exhibit excellent morphology, unambiguous interfaces and well-ordered arrangement. These characteristics were achieved by adjusting the control parameters in the growth process, including the gas flow rate, temperature and pressure. The synthesized GQDs were shown to possess a thickness-dependent photoluminescence (PL) feature. Broad and red-shift emission features in monolayer GQDs suggest that the inhomogeneity of the surfaces, shapes and edges in the quantum dots of the nearby one-layer thickness sensitively affect the PL spectra. However, the GQDs with a thickness of more than 10 layers emit very sharp PL spectra with nearly identical shape and position independent of the excitation wavelength. The results suggest routes towards creating large-scale optoelectronic devices in solid-state white-light emission, photovoltaic solar cells, and flat panel displays.

1. Introduction

Quantum dots (QDs) are currently one of the most active research topics in the fields of material science, photovoltaics and cell biology because of their unique characteristics with a tunable bandgap, large optical absorptivity, sensitive bioimaging and biosensing.[1–3] However, a bottle-neck to the development of QDs is the known toxicity (*e.g.* CdSe and CdTe), high prices and strict synthesis conditions. Correspondingly, carbon QDs are an alternative to traditional semiconductor QDs due to their non-toxicity, biocompatibility, and luminescence. Graphene quantum dots (GQDs) have attracted great interest due to their superior physical properties with wider and more potential applications. Obtaining luminescence from GQDs is very attractive owing to their promising applications in flat-panel displays and LEDs particularly in the visible range. However, the fabrication of GQDs is usually limited by the required special equipment, low yield, uncontrollable sizing and time-consuming processes.[4–9] It is desirable to prepare GQDs with cheap and commercially available methods to obtain a size-controllable batch of products. Chemical vapor deposition (CVD), a relatively economical and versatile technique for producing large amounts of graphene, is regarded as the most promising avenue. Graphene has been grown on a large number of metal substrates by CVD methods, but it is still a great challenge to directly synthesize it on insulators. As described in reports,[10–12] we have developed a graphene CVD growth process on hexagonal boron nitride (h-BN) insulating substrates. In this paper, we first report a facile one-step direct synthesis of GQDs from the decomposition of methane on an h-BN substrate without using any metal catalyst and then present their PL emissions that are directly associated with the thickness of the GQDs. Although the PL properties of size-dependent carbon dots have been reported,[13–15] studies concerning the thickness-dependent PL properties of GQDs obtained by CVD methods remain scarce.

2. Experimental

The synthesis of GQDs was carried out by chemical vapor deposition (CVD) on h-BN substrates by controlling the methane flow rate and the reaction pressure at different temperatures. The fundamental mechanism for GQDs prepared on an h-BN substrate by a CVD procedure is illustrated in Fig. 1. In a typical procedure, the GQDs were directly synthesized on h-BN substrates by atmospheric pressure chemical vapor deposition without any metal catalyzer. The insulator h-BN substrates were placed into a furnace and heated to 1000 °C under the protection of atmospheric argon gas. A mixture of methane and hydrogen gases was then flowed through the furnace, while the argon gas was kept on flowing during the whole experimental process as the carrier gas. To obtain different graphene quantum dots thicknesses, $CH_4 : H_2 : Ar =$ 30 : 60 : 180, 40 : 80 : 200, and 50 : 100 : 200 were adopted to adjust the thickness of the quantum dots while fixing the

[a]School of Materials Science and Engineering, Tongji University, 4800 Caoan Road, Shanghai 201804, P.R. China. E-mail: xuli.rende@163.com; Tel: +86-21-54741714
[b]Department of Physics and Astronomy, Seoul National University, Gwanak-ro, Gwanak-gu, Seoul 151-747, Korea

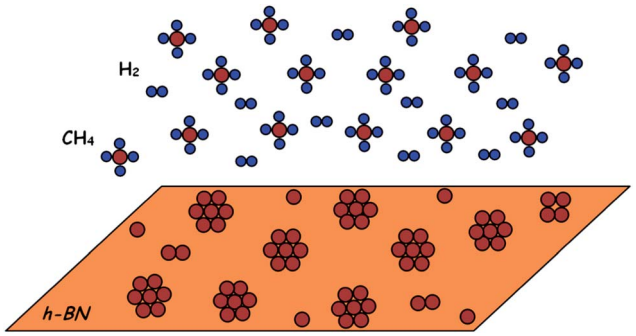

Fig. 1 Schematic representation of CVD growth of GQDs on h-BN substrate.

growth time at 40 min. The average thickness and diameter of the GQDs were determined by repeated AFM (Digital Instrument Dimension 3100, Vecco) measurements with a touching mode to obtain the final quantitative values between the AFM tip and the substrates. The Raman (ThermoFisher, 532 nm laser excitation, 10 mW power) spectra were adopted to further characterize the quality and the number of layers of the obtained samples. X-ray photoelectron spectra (XPS) were measured in a PHI 5000C ESCA system with C1s = 284.6 eV as the benchmark for the binding energy correction. The PL spectra were recorded on a Hitachi 7000 fluorescence spectrophotometer. The detection of PL spectrum was carried out at room temperature, and the samples were excited using a tunable excitation wavelength (200–2200 nm). The luminescence was resolved with a monochromator equipped with a 1200 grooves per mm grating blazed at 1.5 μm.

3. Results and discussion

To investigate their morphology, the synthesized samples were characterized by atomic force microscopy (AFM). In Fig. 2 we present the typical AFM images of GQDs synthesized on h-BN substrates where the smooth and planar surfaces of the h-BN are clearly visible. As indicated in the height profiles in Fig. 2, the average diameter of the prepared GQDs was 80 ± 2 nm for all the samples (Fig. 2(a–c)) used in this work. It was found that the obtained GQDs consisted mainly of homogenous nanosheets. Owing to the special planar characteristics of the h-BN substrates, the GQDs prepared in this work exhibited a very good distribution and arrangement on the surface of h-BN. Moreover, the number of layers and sizes for different samples were verified by the AFM height profile curves, as depicted in the plots at the bottom of each figure in Fig. 2, where the profiles along the white lines clearly show the steps with a thickness of about one layer (Fig. 2(a)), 2–3 layers (Fig. 2(b)), and a few layers (~10 layers, Fig. 2(c)). Fig. 2(d–f) show the topographic height distribution of the GQDs; for each sample, more than 80% of the GQDs had similar thickness. The growth mechanism for graphene quantum dots synthesized on h-BN as described in our previous work[10,12] is mainly epitaxial growth.

Raman spectra, as shown in Fig. 3(a), were used to further confirm the number of layers and the high degree of crystallinity of the synthesized samples. As indicated in Fig. 3(a), a G band at 1590 cm^{-1} and a D band at 1350 cm^{-1} were observed despite the accompanying very sharp and strong characteristic peak of h-BN around 1367 cm^{-1}. Unlike the GQDs synthesized with previously reported methods,[7,13–18] the 2D band for the samples in this work was relatively high, similar to that of high-quality larger-area graphene; the ratio of the intensity of the 2D band to that of the G band was close to 2 for monolayer GQDs, 0.9 for 2–3-layered GQDs and 0.5 for GQDs with a few layers. These features indicate that the GQDs synthesized in this work have not only high quality but also high surface density of the dots, which shows the uniqueness of the h-BN substrate-based CVD method developed here for GQD preparation.

X-ray photoelectron spectroscopy (XPS) was carried out to investigate the microstructure and composition of the as-synthesized GQDs samples. As shown in Fig. 3(b), the XPS spectra exhibited an obvious C1s peak at 285.0 eV from the as-prepared GQDs and a B1s peak at 189.2 eV and an N1s peak at 398.4 eV from the h-BN substrate, as well as an O1s peak at 533 eV. In the XPS results, the C1s peak at 285.0 eV as shown in the inset of Fig. 3(b) indicated the graphitic sp^2 carbon signal for the as-synthesized GQDs on the h-BN surfaces, which is consistent with the value for the C–C bond as indicated in ref. 18. The higher C1s peak relative to the corresponding O1s peak seen for the GQDs (few-layer) compared to the monolayer GQDs suggested that oxygen absorption on the surface of GQDs occurred during the CVD preparation of GQDs.

The carbon quantum dots could be made luminescent by inducing a bandgap through a reduction of the connectivity of the π-electron network. The luminescence properties of the obtained GQDs were further explored. Remarkably, the quantum dots exhibited excellent PL properties along with strong luminescence in the visible range as shown in Fig. 4(a–c). The PL spectra exhibited an excitation-dependent feature that was similar to that reported in previous studies.[13,14,18–20] Increasing the excitation wavelength also led to a longer emission wavelength; both the emission peak positions and the peak intensities of GQDs varied when they were excited at different excitation wavelengths. Even though different luminescence mechanisms have been proposed by several groups,[4,13,21–24] further work is necessary to reveal the intrinsic origins of luminescence for GQDs. It is important to note that the CVD process that we developed does not involve complex chemicals, in contrast to the previous reports. GQDs made by this CVD method have a cleaner and purer chemical composition than those in the previous reports. Therefore, the GQDs synthesized by CVD can further reflect the nature of luminescence of the carbon quantum dots. The most interesting finding in this work is the observation of the novel PL behavior that the PL emission spectra of the GQDs exhibit thickness-dependent features. As the thickness of GQDs was increased from 1 layer to 2–3 layers and towards more than 10 layers, we observed a distinct decrease in the full width at half maximum (FMHM) of the emission peak, with a significant change in the shape. Increasing thickness in the basic range to more than 10 layers led to the disappearance of the 370 nm shoulder peak and the

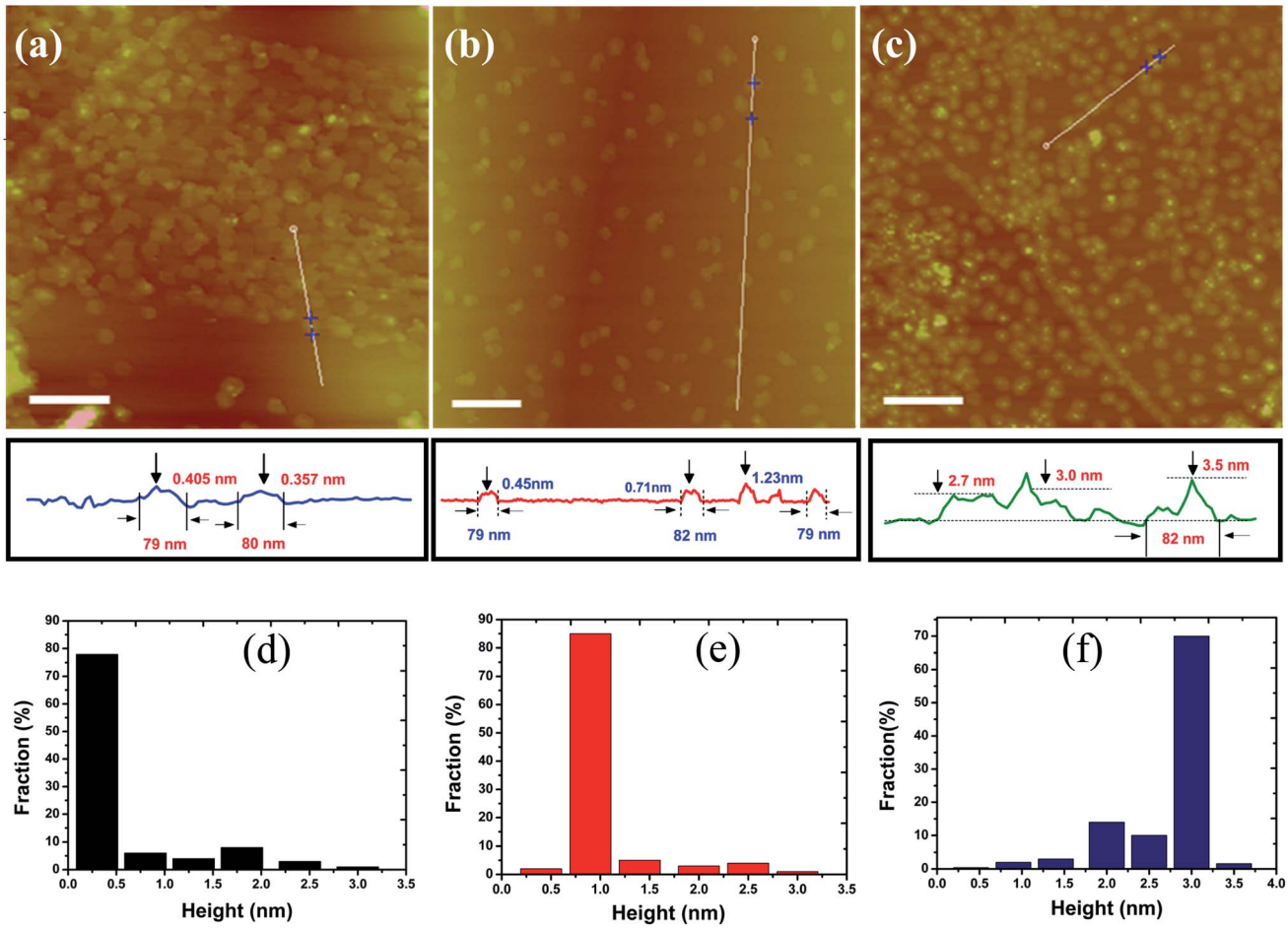

Fig. 2 AFM images of GQDs on h-BN substrates with width and height profiles along the white lines in the images at the corresponding lower parts for (a–c): (a) monolayer GQDs, (b) bilayer GQDs, and (c) few-layer GQDs. (d–f) Height distribution of the GQDs corresponding to (a)–(c). Height ≤0.5 nm, monolayer; ≤1.2 nm, bilayer; ≤3.5, ten-layer. The scale bars in a, b, and c are 200 nm.

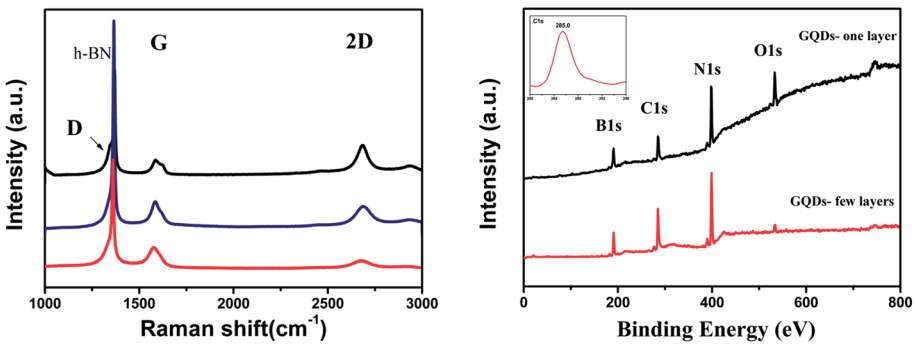

Fig. 3 (a) Raman spectra for GQDs with different thicknesses on h-BN substrates: monolayer GQDs (black); bilayer GQDs (red); few-layer GQDs (blue). (b) XPS spectrum of GQDs on h-BN substrate. Inset shows the C1s peak.

appearance of two sharp peaks near 420 and 470 nm. Analysis of the data in Fig. 4(a–c) for GQDs with different thicknesses revealed a more complex PL emission mechanism than that reported previously.[13,21–23] For monolayer GQDs, we observed that the 420 nm emission was efficiently induced by 340 nm excitation, but when the sample was adjusted to nearly 10 layers, the strongest emission with an excitation wavelength of 400 nm was emitted at 450 nm. Due to the large surface-to-volume ratio of the graphene nanomaterial, not only different sizes in the 2D plane but also different thicknesses of the quantum dots sensitively affect the PL properties. The monolayer GQDs are very sensitive to the excitation wavelength, where the FWHM is broadened and emission peak is red-shifted as the excitation wavelength is increased. Broad-band room

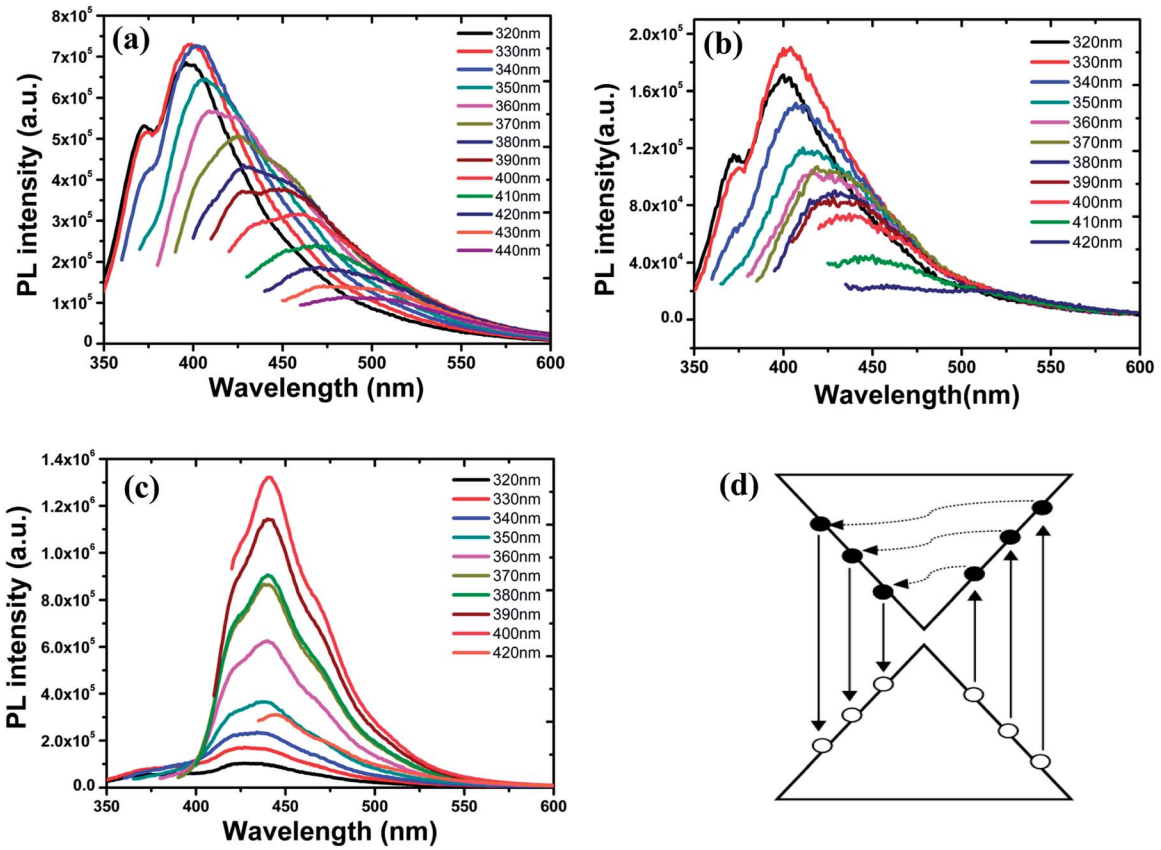

Fig. 4 (a) PL spectra of monolayer GQDs. (b) PL spectra of bilayer GQDs. (c) PL spectra of few-layer GQDs. (d) Schematic representation of photoexcited electron kinetics in linear band dispersion for monolayer GQDs.

temperature photoluminescence may arise from the radiation of excitations from the non-equilibrium states. The photoexcited carriers with a transition from the valence to the conduction band were scattered by phonons from the lattice vibration before recombination took place accompanied by photon emission. The emission spectra throughout the visible spectrum range appeared to have energy lower than the exciting one due to the electron energy loss in inelastic scattering.

The layer-dependent PL properties may also be explained by the linear dispersion relation of the valence and the conduction bands that intersect at the Dirac point. The linear dispersion of the electron energy bands implied that for any excitation there will always be an electron–hole pair in resonance; the photoexcited electron kinetics in the linear energy level dispersion for the one-layer GQDs is shown in Fig. 4(d). For both one-layer and ten-layer GQDs, a small energy gap can be opened between the valence and the conduction band due to the quantum confinement effects. However, when the quantum dot thickness is more than 10 atom layers, the GQDs become common graphite C-dots and the energy level dispersion near the Dirac point recovers to the parabolic-type band structure. The excitation and radiative recombination in the quasi-continuous energy states in the thicker C-dots are likely to be responsible for the progressively narrowing PL emission, as observed in Fig. 4(c). At the same time, the monolayer GQDs likely have more variable emission sites or surface states on the quantum islands, which leads to the broadening and red-shift radiative recombination of excitations from not only different sizes of GQDs in the samples but also a distribution of different emissive trap sites. The thicker quantum dots are more like the graphite dots; the narrowing PL bands can be attributed to the carrier redistribution within the ensemble of samples. All these factors may be the causes of the diverse layer behavior of the PL bands, as shown in Fig. 4(a–c). In addition, the surface dot density is also a key issue to control the whole PL intensity. The less intense PL indicated in Fig. 4(b) was assigned to a lower surface quantum dot density, which can be confirmed further through Fig. 2(b) as compared with the dot density shown in Fig. 2(a) and (c). The higher the quantum dot density is, the stronger is the luminescence intensity. Therefore, layer-controllable GQDs can be particularly valuable for emission with multiple colors, particularly in the case of solid white light emission. Although some suppositions about the luminescence mechanism of the GQDs have been proposed, including quantum-confinement effects, its origin is still not clear. However, whatever the origin, the fluorescent inorganic and non-toxic carbon-based semiconductors are of particular importance for low-cost optoelectronics, ranging from light-emitting devices and solar cells to photodetectors, touch screens and flexible smart windows. In addition, bio-compatible carbon-based fluorescent quantum dots are a better alternative to the traditional semiconductor QDs for bio-imaging and bio-labelling.

4. Conclusions

In summary, we successfully fabricated GQDs on h-BN substrates without using any metal catalyst by chemical vapor deposition. The PL properties of GQDs with different layers were investigated. We found strongly thickness-dependent visible PL characteristics from the CVD synthesized GQDs. Relatively broad and red-shifted emission features appeared in the case of monolayer GQDs, while sharp and nearly identical emissions with different excitation wavelengths appeared in the case of thick GQDs. It was demonstrated that these GQDs have tunable luminescence properties controlled by the thickness of graphene layers. The results presented here offer a new route of preparing batches of commercially available graphene nanomaterials by a simple and easy method which is promising for the development of new active materials in the field of optoelectronics. Moreover, our results will promote further studies on the application of GQDs due to the advantage of the CVD method that provides a high-density integration of high-quality GQDs. GQDs orderly arranged over a large area enable the large-scale fabrication of flexible and transparent optoelectronic devices in solar cells, LEDs, and flat panel displays.

Acknowledgements

This work was supported by research funding from the Chinese Academy of Science (Grant no. KGCX2-YW-231), the Science and Technology Commission of Shanghai Municipality (Grant no. 10DJ1400600), and the National Science and Technology Major Project (Project no. 2011Zx02707). We also thank the Momentive Company from the U.S. for providing the h-BN single crystal.

References

1 P. O. Anikeeva, J. E. Halpert, M. G. Bawende, *et al.* Quantum dot light-emitting devices with electroluminescence tunable over the entire visible spectrum, *Nano Lett.*, 2009, **9**, 2532–2536.
2 E. H. Sargent, Infrared photovoltaics made by solution processing, *Nat. Photonics*, 2009, **3**, 325–331.
3 X. Wu, H. Liu, J. Liu, K. N. Haley, J. A. Treadway, J. P. Larson, *et al.* Immunofluorescent labeling of cancer marker Her2 and other cellular targets with semiconductor quantum dots, *Nat. Biotechnol.*, 2003, **21**, 41–46.
4 Y. P. Sun, B. Zhou, Y. Lin, W. Wang, K. A. S. Fernando, P. Pathak, *et al.* Quantum-Sized Carbon Dots for Bright and Colorful Photoluminescence, *J. Am. Chem. Soc.*, 2006, **128**, 7756–7757.
5 L. Y. Zheng, Y. W. Chi, Y. Q. Dong, J. P. Lin and B. B. Wang, Electrochemiluminescence of Water-Soluble Carbon Nanocrystals Released Electrochemically from Graphite, *J. Am. Chem. Soc.*, 2009, **131**, 4564–4565.
6 R. L. Liu, D. Q. Wu, S. H. Liu, K. Koynov, W. Knoll and Q. Li, An Aqueous Route to Multicolor Photoluminescent Carbon Dots, *Angew. Chem., Int. Ed.*, 2009, **48**, 4598–4601.
7 J. Peng, W. Gao, B. K. Gupta, Z. Liu, R. Romero-Aburto, L. Ge, *et al.* Graphene Quantum Dots Derived from Carbon Fibers, *Nano Lett.*, 2012, **12**, 844–849.
8 Y. Yang, J. Cui, M. Zheng, C. Hu, S. Tan, Y. Xiao, *et al.* One-step synthesis of amino-functionalized fluorescent carbon nanoparticles by hydrothermal carbonization of chitosan, *Chem. Commun.*, 2012, **48**, 380–382.
9 L. Tang, R. Ji, X. Cao, J. Lin, H. Jiang, *et al.* Deep Ultraviolet Photoluminescence of Water-Soluble Self-Passivated Graphene Quantum Dots, *ACS Nano*, 2012, **6**, 5102–5110.
10 X. Ding, G. Ding, X. Xie, F. Huang and M. Jiang, Direct growth of few layer graphene on hexagonal boron nitride by chemical vapor deposition, *Carbon*, 2011, **49**, 2522–2525.
11 X. Ding, H. Sun, X. Xie, H. Ren, F. Huang and M. Jiang, Anomalous paramagnetism in graphene on hexagonal boron nitride substrates, *Phys. Rev. B: Condens. Matter Mater. Phys.*, 2011, **84**, 174417.
12 S. Tang, G. Ding, X. Xie, J. Chen, C. Wang, X. Ding, *et al.*, Nucleation and growth of single crystal graphene on hexagonal boron nitride, *Carbon*, 2012, **50**, 329–331.
13 D. Pan, J. Zhang, Z. Li and M. Wu, Hydrothermal Route for Cutting Graphene Sheets into Blue-Luminescent Graphene Quantum Dots, *Adv. Mater.*, 2010, **22**, 734–738.
14 Y. Li, Y. Hu, Y. Zhao, G. Shi, L. Deng, Y. Hou, *et al.* An Electrochemical Avenue to Green-Luminescent Graphene Quantum Dots as Potential Electron-Acceptors for Photovoltaics, *Adv. Mater.*, 2011, **23**, 776–780.
15 D. Pan, L. Guo, J. Zhang, C. Xi, Q. Xue, H. Huang, *et al.* Cutting sp^2 clusters in graphene sheets into colloidal graphene quantum dots with strong green fluorescence, *J. Mater. Chem.*, 2012, **22**, 3314–3318.
16 Y. Li, Y. Zhao, H. Cheng, Y. Hu, G. Shi, L. Dai, *et al.* Nitrogen-Doped Graphene Quantum Dots with Oxygen-Rich Functional Groups, *J. Am. Chem. Soc.*, 2012, **134**, 15–18.
17 X. Yan, X. Cui, B. Li and L.-S. L. Large, Solution-Processable Graphene QuantumDots as Light Absorbers for Photovoltaics, *Nano Lett.*, 2010, **10**, 1869–1873.
18 Y. Sun, S. Wang, C. Li, P. Luo, L. Tao, Y. Wei and G. Shi, Large scale preparation of graphene quantum dots from graphite with tunable fluorescence properties, *Phys. Chem. Chem. Phys.*, 2013, **15**, 9907–9913.
19 R. Liu, D. Wu, X. Feng and K. Müllen, Bottom-Up Fabrication of Photoluminescent Graphene Quantum Dots with Uniform Morphology, *J. Am. Chem. Soc.*, 2011, **133**, 15221–15223.
20 L. Bao, Z.-L. Zhang, Z.-Q. Tian, L. Zhang, C. Liu, Y. Lin, *et al.* Electrochemical Tuning of Luminescent Carbon Nanodots: From Preparation to Luminescence Mechanism, *Adv. Mater.*, 2011, **23**, 5801–5806.
21 H. Li, X. He, Z. Kang, H. Huang, Y. Liu, J. Liu, *et al.* Water-soluble fluorescent carbon quantum dots and photocatalyst design, *Angew. Chem., Int. Ed.*, 2010, **49**, 4430–4434.
22 Q. L. Zhao, Z. L. Zhang, B. H. Huang, J. Peng, M. Zhang and D. W. Pang, Facile preparation of low cytotoxicity fluorescent carbon nanocrystals by electrooxidation of graphite, *Chem. Commun.*, 2008, 5116–5118.

23 G. Eda, Y.-Y. Lin, C. Mattevi, H. Yamaguchi, H.-A. Chen, I.-S. Chen, *et al.* Blue Photoluminescence from Chemically Derived Graphene Oxide, *Adv. Mater.*, 2010, **22**, 505–509.

24 R. Zhao, J. Wang, M. Yang, Z. Liu and Z. Liu, Graphene quantum dots embedded in a hexagonal BN sheet: identical influences of zigzag/armchair edges, *Phys. Chem. Chem. Phys.*, 2013, **15**, 803–806.